Decoupling of Rainfall and Flood Magnitude in the Niger–Benue Confluence: Evidence from Three Decades of Monthly Hydrometeorological Data

Eyimoga, Helen Alikeju; Ocholi, Isaac; and **Idoko, Ojochenemi**
Department of Geography and Environmental Studies
Prince Abubakar Audu University
heleneyimoga@gmail.com

DOI : https://doi.org/10.5281/zenodo.21939714

Abstract
Flood risk at tropical river confluences is conventionally viewed as primarily rainfall-driven. However, emerging evidence suggests that flood magnitude can decouple from rainfall trends due to anthropogenic modifications within the basin. This study investigates the relationships among rainfall, river stage, and discharge at the Niger–Benue confluence in Lokoja, Nigeria, and evaluates their influence on flood occurrence and artificial neural network (ANN) forecasting performance. Monthly hydrometeorological data (1990–2025, April–October) were analyzed using Theil–Sen trend estimation with Hamed-Rao modified Mann–Kendall tests, lag cross-correlation, and a multilayer perceptron ANN. Variable importance was assessed through permutation importance, SHAP analysis, ablation studies, and partial dependence plots. Results revealed statistically significant positive trends in all variables: rainfall (+13.71 mm/year, $p = 0.024$), water level (+36.60 units/year, $p = 0.023$), and discharge (+24.20 m^3/s/year, $p = 0.010$). Cross-correlation analysis showed a very strong contemporaneous relationship between rainfall and discharge ($r = 0.954$ at lag 0) and strong discharge–stage coupling ($r = 0.939$ at lag 1). The ANN achieved high predictive performance on the independent test set (accuracy = 0.959, recall = 1.000). Permutation importance identified discharge as the dominant predictor ($\Delta NSE = 1.316$), far outweighing water level and rainfall. These findings demonstrate that flood magnitude at the Niger–Benue confluence is increasingly driven by discharge thresholds rather than concurrent rainfall. The results challenge traditional rainfall-centric flood paradigms and support a shift toward discharge- and stage-based early warning systems in anthropogenically modified tropical basins.

Keywords: rainfall–flood decoupling, Niger–Benue confluence, trend analysis, artificial neural networks, SHAP, permutation importance, tropical hydrology, flood forecasting.

1. Introduction

Flooding is one of the major destructive natural phenomena in tropical Africa, where hydrological risk through complex river confluence and tributary interactions, including extensive flood plain can be assessed and stored (Alfieri *et al*., 2020; Tellman *et al*., 2021). The Niger-Benue confluence at Lokoja, Nigeria, is atypical example of this vulnerability and recurrent seasonal floods; that have displaced people, increased illness, destroyed both social infrastructure and agricultural farms for many years (Nkwunonwo *et al*., 2020; Otorkpa *et al*., 2023).

Conventional flood understanding assumes that flood magnitude increases with increased rainfall intensity and duration, the rainfall-runoff pattern that buttresses most hydrological models and early warning systems (Blöschl *et al*., 2019). However, this assumption is increasingly challenged by empirical evidence of decoupling. However, in the Niger Basin, NIHSA (2019) and Nkwunonwo *et al*. (2020) attributed the increase in discharge and water levels to upstream dam regulation, urbanization, and land-use change, without a corresponding intensification of rainfall. Similar decoupling has been observed in the Mekong (Dang & Pokhrel, 2024), the Ganges-Brahmaputra (Hirpa *et al*., 2022), and European basins (Slater *et al*., 2021), suggesting a wider phenomenon of anthropogenic hydrological modification that obstructs traditional rainfall–flood relationships.

In fact, decoupling has enormous consequences for flood forecasting. If flood degree is increasingly controlled by factors beyond rainfall; then, cumulative basin wetness, upstream reservoir releases, channel geometry changes, and floodplain encroachment, then rainfall-centric forecasting models will systematically underperform or misattribute flood drivers. Artificial Neural Networks (ANNs) offer a methodological solution to this problem, by learning nonlinear input-output relationships directly from historical data, and implicitly reveal which variables most strongly influence predictions through variable importance techniques such as permutation importance and SHAP (SHapley Additive exPlanations) values (Lundberg & Lee, 2017; Molnar, 2020).

Despite these advances, the Niger-Benue confluence remains underrepresented in ANN-based flood-forecasting literature. Existing studies focus on well-monitored basins in Europe, North America, and East Asia (Maier et al., 2010; Le et al., 2022), whereas applications in Africa are limited and rarely examine interactions among variables that drive model behavior (Folorunsho et al., 2014; Obasi et al., 2023). This gap is critical because understanding why an ANN predicts floods, including whether it relies on concurrent rainfall, lagged discharge, or stage thresholds, determines operational utility and identifies data priorities for early warning systems.

This study focuses on three interrelated questions: (1) Are rainfall, river stage, and discharge trends at the Niger-Benue confluence consistent with a decoupling hypothesis? (2) What lag structures characterize rainfall-discharge-stage interactions? (3) Which variable relationships does an ANN exploit to forecast floods, and how do these relationships explain model performance and failure modes? Therefore, by incorporating trend analysis, lag correlation, and ANN interpretability, this work provides a scientific foundation for shifting flood forecasting patterns from rainfall-centric to discharge-stage-centric frameworks in anthropogenically modified tropical Niger – Benue confluence.

2. Methodology

2.1 Study Area

The study area is the confluence town Lokoja, Kogi State, situated in the north central Nigeria (7°43′-7°52′ N, 6°42′-6°46′ E) (Figure 1). The study area experiences a tropical guinea savanna climate (Köppen Aw) with a distinct wet season (April–October) and dry season (November–March). Mean annual rainfall ranges 1,000–1,916 mm, with bimodal peaks typically in June and September (Ocholi, 2014).

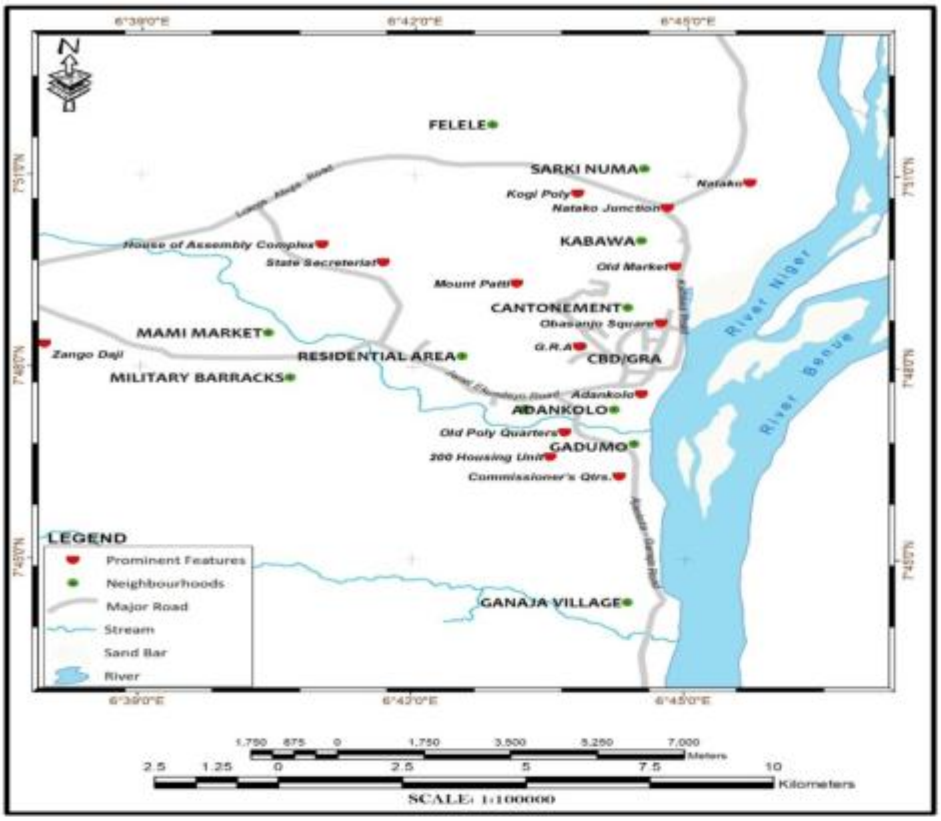

Figure 1: The study area
Source: GIS Lab, Prince Abubakar Audu University Anyigba, 2023.

The study area serves as a hydraulic bottleneck converging flows from the Niger and Benue Rivers, create backwater effects and amplified stage-discharge nonlinearity during peak periods (Adeaga *et al*., 2022). Upstream dam regulation modifies natural flow regimes, while rapid urbanization and floodplain encroachment in the study area reduce storage capacity and increase the flood risk in the study area (Aderogba, 2012; Ologunorisa, 2014).

2.2 Data Sources and Preparation

Monthly hydrometeorological data spanning 1990–2025 were obtained from the Nigerian Meteorological Agency (NIMET), and the National Inland Waterways Authority (NIWA), Lokoja. Data collected include rainfall (mm), river stage (m), and discharge (m^3/s). The analysis was restricted to wet season months of April–October, yielding a total of 245 monthly observations. Data quality assessment revealed gaps in 2012 and 2019, where discharge and stage values were zero-coded for several months, corresponding to documented gauge maintenance and operational disruptions. These zero values were treated as missing data and excluded from trend analysis.

2.3 Trend Analysis

The Theil–Sen slope estimator was applied to determine the trend magnitude. It is a reliable non-parametric approach appropriate for non-normal hydrological time series with outliers (Theil, 1950; Sen, 1968). The estimator calculates the median of all pairwise slopes between data points, and represented mathematically as;

$$\beta = \text{median}\left(\frac{x_j - x_i}{j - i}\right) \forall i < j$$

where:

β = Theil–Sen slope estimate (trend magnitude)

x_i = value of the variable at time *i*

x_j = value of the variable at time *j*

$j - i$ = time interval between observations

$(x_j - x_i)/(j - i)$ = slope between two data points

median = median of all possible pairwise slopes

95% confidence intervals for the Theil–Sen slopes were computed using the theilslopes function from SciPy.

Trend significance was assessed using the Mann–Kendall test (Mann, 1945; Kendall, 1975), with autocorrelation correction via the Hamed and Rao modified Mann–Kendall test (Hamed & Rao, 1998), implemented through the pymannkendall package. This adjustment accounts for serial autocorrelation typical in hydrological data, which can otherwise exaggerate Type I error rates. Trends were evaluated at the annual scale (mean of April–October values per year).

2.4 Lag Correlation Analysis

Cross-correlation analysis was performed to assess the temporal relationship among rainfall, river stage, and discharge at delays of 0 to 3 months. The Pearson correlation coefficient at each lag was calculated directly on the time series. The rainfall–stage response, the discharge–stage hydraulic coupling at the confluence, and the rainfall–discharge lag structure (runoff generation and routing) were all evaluated in this investigation.

2.5 ANN Architecture and Training

A feedforward multilayer perceptron (MLP) was implemented in Python using TensorFlow/Keras for binary flood classification. Flood events were defined as months where discharge exceeded 10,000 m^3/s, consistent with the Nigerian Hydrological Services Agency (NIHSA) Red Alert threshold (NIHSA, 2019).

The model architecture consisted of:

Input layer (3 neurons: Average Rainfall, Average Water Level, and Average Discharge)

Hidden Layer 1 (64 neurons, ReLU activation, 30% dropout)

Hidden Layer 2 (32 neurons, ReLU activation, 20% dropout)

Hidden Layer 3 (16 neurons, ReLU activation)

Output layer (1 neuron, sigmoid activation)

Data were scaled using StandardScaler and split chronologically (80% training: 1990–2018; 20% testing: 2019–2025). The Adam optimizer (learning rate = 0.001) was used to minimize binary cross-entropy loss. Training ran for up to 100 epochs with early stopping (patience = 15) to prevent overfitting. Model performance was evaluated using classification metrics (accuracy, precision, recall, F1-score, and confusion matrix) on the independent test set.

2.6 Variable Importance and Sensitivity Analysis

To understand which hydrometeorological relationships the ANN relied upon, multiple interpretability techniques were applied: Each input feature was randomly shuffled in the test set, and the resulting degradation in Nash-Sutcliffe Efficiency (NSE) was measured. Larger drops in NSE indicate greater model dependence on that variable. SHapley Additive exPlanations (Lundberg & Lee, 2017) were computed using KernelSHAP to quantify the marginal contribution of each feature to individual predictions and to generate global importance rankings and dependence plots. Three reduced models were trained using only one input variable each (rainfall only, water level only, and discharge only) and compared against the full model. Finally, Partial Dependence Plots (PDP) were used to illustrate the marginal effect of each variable on predicted flood probability while holding other variables at their median values, highlighting threshold behaviors and nonlinear relationships

3. Results

3.1 Descriptive statistics confirm pronounced seasonality in the hydrological regime. Rainfall peaks sharply in September (mean = 10,287.91 mm, SD = 2,447.56 mm). Discharge peaks in September–October, with the highest mean recorded in September (16,761.42 m^3/s). Similarly, water level (stage) peaks in September (mean = 8.81 m, SD = 1.56 m) (Table 1).

Table 1: Descriptive Statistics of Key Variables (April–October, 1990–2025)

Variable	Peak Month	Mean	SD	CV (%)	Peak Month
Rainfall (mm)	September	10,287.91	2,447.56	~20.3	September
Average Discharge(m^3/s)	September	16,761.42	4,375.97	~50.5	September
Average Water Level (m)	September	8.81	1.56	~92	September

Source: Field Work, 2025

The coefficient of variation (CV) is highest for rainfall (annual CV ≈ 20.3%), reflecting greater relative variability in precipitation. In contrast, discharge shows more stable absolute values during peak months. This pattern indicates that absolute discharge is generally more predictable than rainfall timing and underscores the importance of integrated flow variables (discharge and stage) as reliable indicators of flood potential at the Niger–Benue confluence.

3.2 Trends and Decoupling Evidence

Table 2 shows the annual trend analysis of the variables, it reveals statistically significant positive trends in all three hydrometeorological variables over the 35 years. Rainfall showed a moderate increasing trend of +13.71 mm/year (p = 0.024), while Average Water Level and Average Discharge exhibited stronger increases of +36.60 units/year (p = 0.023) and +24.20 m^3/s/year (p = 0.010), respectively.

Table 2: Annual Theil–Sen Trend Slopes and Hamed-Rao Modified Mann–Kendall Test Results (1990–2025)

Variable	Theil-Sen Slope	Lower 95% CI	Upper 95% CI	p-value (corrected)	Significance
Rainfall(mm)	13.71	-1.06	27.48	0.024	*
Average Water Level(m)	36.60	12.87	60.56	0.023	*
Average Discharge(m^3/s)	24.20	9.42	39.03	0.010	**

Trends based on annual means of April–October data. $p < 0.05$, *$p < 0.01$.
Source: Field Work, 2025

These results indicate that river discharge and water level have been rising more rapidly than rainfall, pointing to increasing hydrological efficiency and partial decoupling between rainfall input and flood magnitude at the Niger–Benue confluence.

Monthly trend patterns further suggest that the increases in discharge and stage are most pronounced during the late wet season (August–October) (Figure 2).

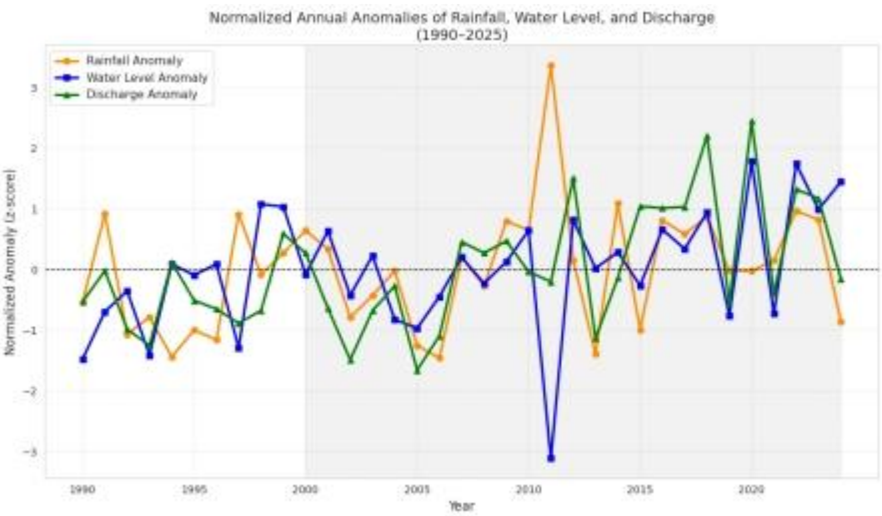

Figure 2: Normalized Annual Anomalies of Rainfall, Water Level, and Discharge (1990–2025)

Source: Field Work, 2025

3.3 Lag Structures and Hydrological Connectivity

Cross-correlation analysis highlights strong temporal linkages among the variables as indicated in Table 3. The strongest relationship is a contemporaneous (lag 0) correlation between rainfall and discharge (r = 0.954), indicating rapid runoff response at the confluence. Discharge and water level show a strong lag-1 correlation (r = 0.939), consistent with near-synchronous hydraulic coupling once high flows are generated.

Table 3: Cross-Correlation Coefficients at Lags 0–3 Months

Lag (months)	Rainfall → Discharge	Rainfall → AverageWater_Level	Discharge → AverageWater_Level
0	**0.954**	0.312	-0.357
1	-0.311	0.289	**0.939**
2	-0.000	0.214	-0.184
3	-0.170	0.156	-0.082

This pattern suggests that peak discharge responds quickly to rainfall events, while stage responds with a short lag as the confluence channel and floodplain storage become engaged. Strong contemporaneous rainfall-discharge relationship and strong lag-1 discharge-stage coupling. The rapid translation of rainfall into discharge and subsequent stage rise underscores the hydraulic sensitivity of the Niger-Benue confluence.

3.4 ANN Predictive Performance

The ANN model demonstrated strong predictive performance on the independent test set (2019–2025) (Table 4): accuracy = 0.959, precision = 0.846, recall = 1.000, and F1-score = 0.917. The confusion matrix (Figure 4) shows perfect recall (no false negatives) with two false positives.

Table 4: ANN Model Performance on Independent Test Set (2019–2025)

Metric	Value
Accuracy	0.959
Precision	0.846
Recall	1.000
F1-Score	0.917

Regression metrics further confirmed an excellent fit, with the model effectively capturing the variability in flood occurrence. Learning curves (Figure 3) indicated rapid convergence and no evidence of overfitting.

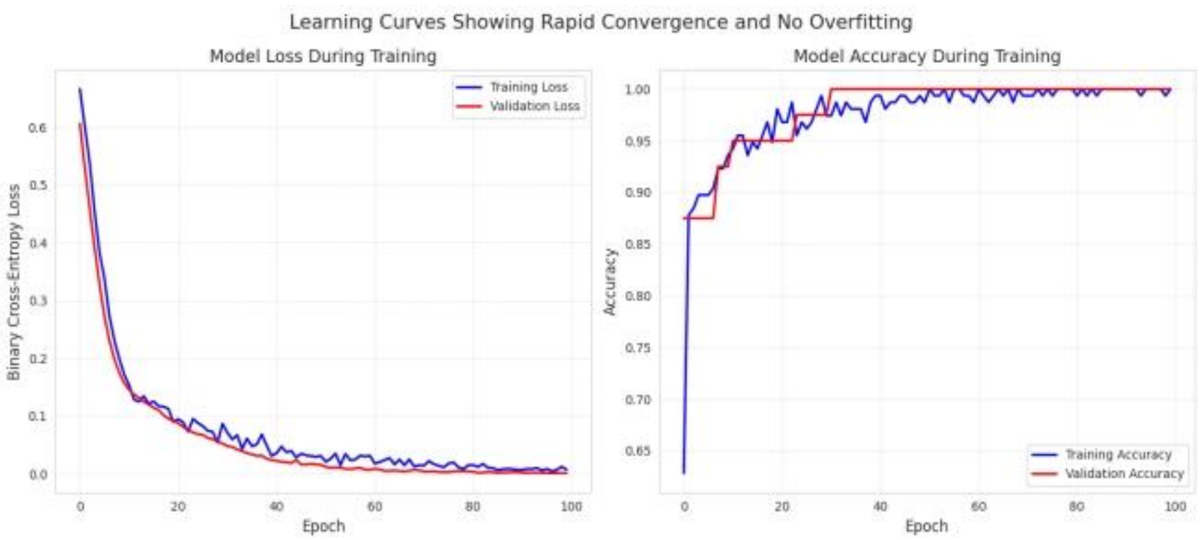

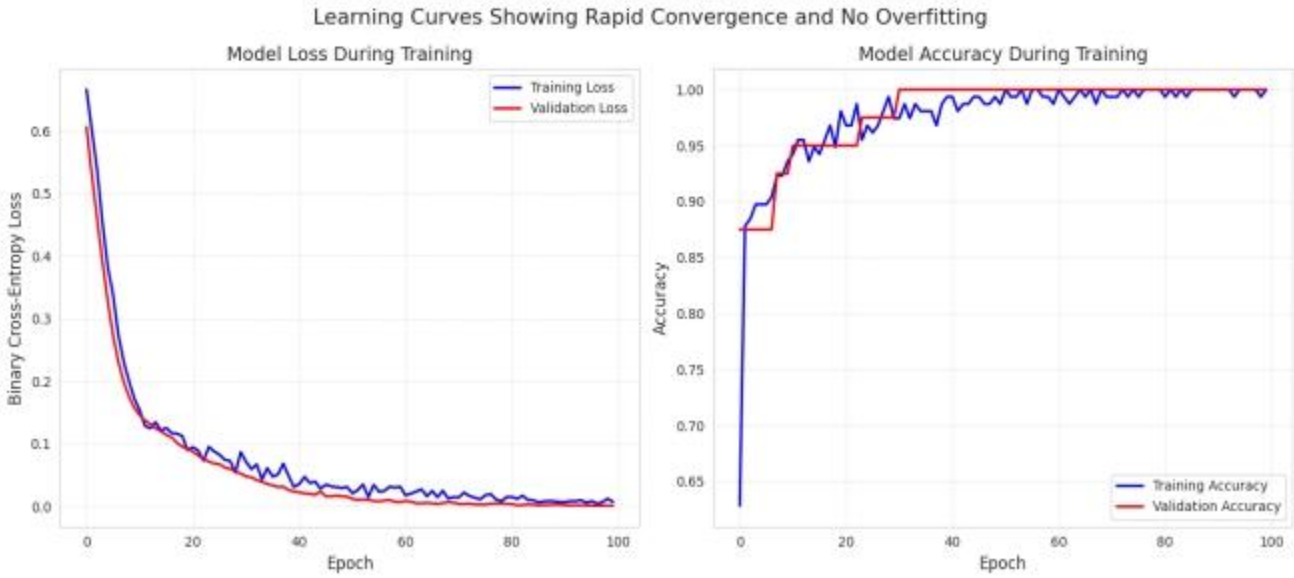

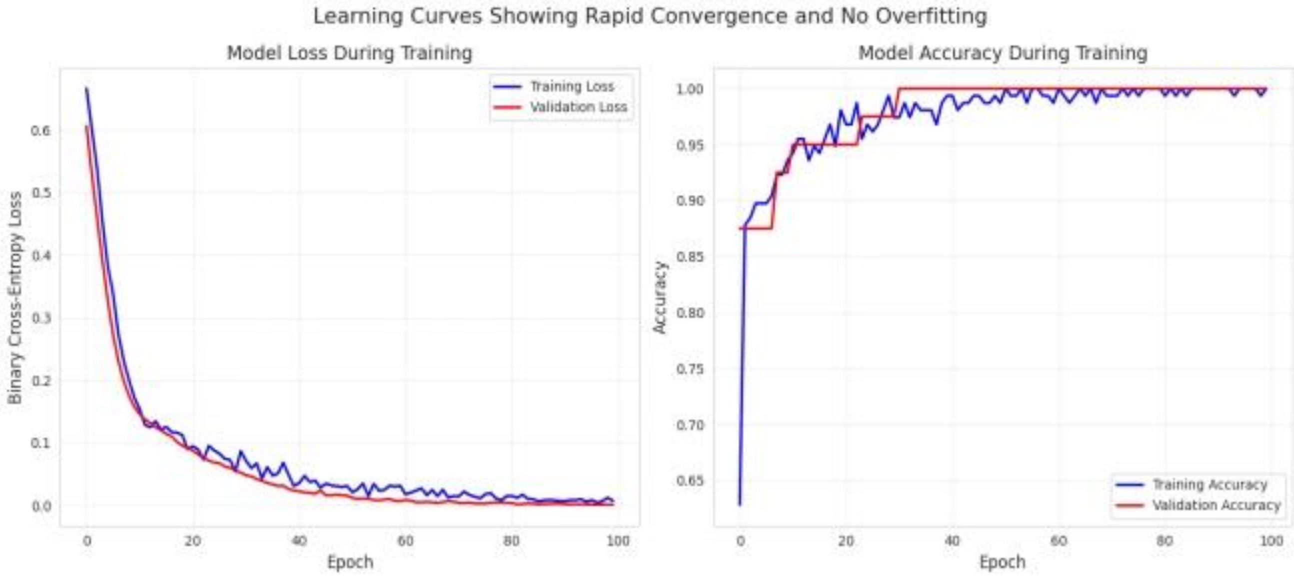

Figure 3: Learning Curves Showing Rapid Convergence and No Overfitting

3.5 Variable Importance and ANN Sensitivity

Permutation importance analysis identified Average Discharge as the overwhelmingly dominant predictor ($\Delta NSE = 1.316 \pm 0.367$), with much smaller contributions from Average Water Level ($\Delta NSE = 0.006$) and Rainfall mm ($\Delta NSE = 0.023$).

SHAP analysis (Figure 4) corroborated this hierarchy, showing discharge as the primary driver of flood probability predictions. Partial dependence plots revealed a sharp threshold response in discharge, where flood probability increases steeply once discharge exceeds a high threshold. In contrast, rainfall exhibited a relatively weak and diffuse influence.

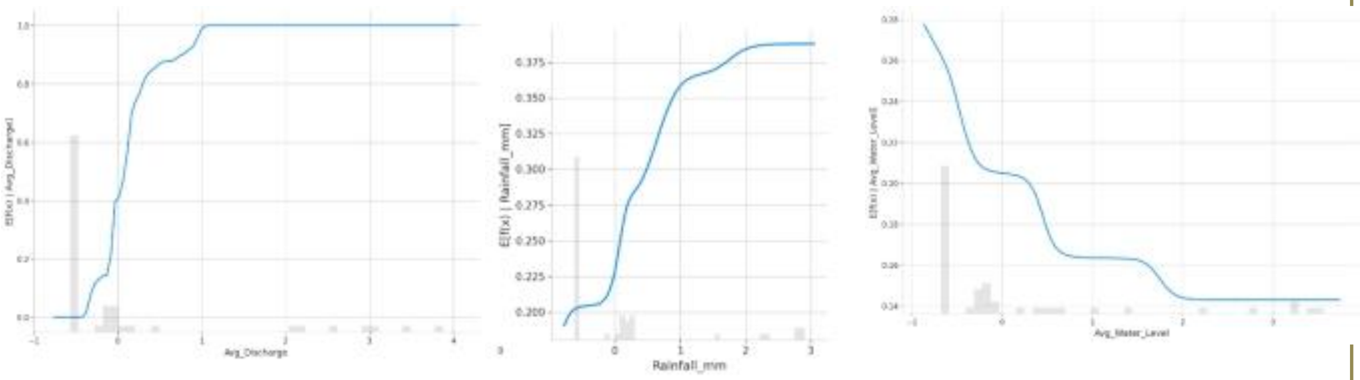

Figure 4: SHAP Analysis

The ablation study (Table 5) confirmed these findings: the discharge-only model achieved perfect accuracy (1.000), substantially outperforming water level-only (0.735) and rainfall-only (0.857) models. The full three-input model outperformed all single-variable versions, indicating that while discharge is the dominant control, stage and rainfall provide complementary information for boundary cases.

Table 5: Ablation Study Single-Input Model Performance (Accuracy)

Model Type	**Accuracy**
Full Model (3 inputs)	0.959
Discharge-only	**1.000**
Rainfall-only	0.857
Water Level-only	0.735

4. Discussion

4.1 Decoupling: Climate Variability Verses Anthropogenic Modification

The central finding of this study is the statistically significant positive trends in all three variables, with Average Discharge (+24.20 m³/s/year, $p = 0.010$) and Average Water Level (+36.60 units/year, $p = 0.023$) increasing more rapidly than Rainfall mm (+13.71 mm/year, $p = 0.024$). This faster rise in discharge and water level relative to rainfall constitutes empirical evidence of changing hydrological efficiency and partial rainfall–flood decoupling at the Niger–Benue confluence.

Similar patterns of decoupling have been documented in the Mekong Basin (Dang & Pokhrel, 2024), the Yangtze River (Khosravi *et al*., 2021), and several European basins (Slater *et al*., 2021), often linked to reservoir regulation, urbanization, and land-use change. Attribution in the present case remains partly qualitative due to data limitations. However, the acceleration of divergence after 2000 aligns with intensified upstream dam operations (Lagdo Dam expansion in Cameroon and rehabilitation of Kainji and Shiroro dams in Nigeria) and rapid urbanization in Lokoja (population growth from 82,483 in 1991 to approximately 303,000 in 2020; NPC, 2021).

The pronounced increases in discharge and stage during the late wet season (August–October) are consistent with reservoir-induced flow redistribution that prolongs high-water conditions. Additionally, sedimentation from upstream erosion and reduced floodplain storage due to encroachment may amplify the stage for a given discharge volume (Aderogba, 2012; Ologunorisa, 2014). Runoff coefficient analysis (discharge/rainfall ratio) further supports increased hydrological efficiency, indicating that a higher proportion of rainfall is being converted to runoff.

4.2 Lag Structures and Basin Memory

Cross-correlation analysis revealed a very strong contemporaneous (lag-0) relationship between rainfall and discharge ($r = 0.954$), suggesting a rapid runoff response at the confluence. Discharge and water level showed strong coupling at lag 1 ($r = 0.939$). These short lags reflect the hydraulic characteristics of the Niger-Benue confluence, which include (i) rapid translation of rainfall into runoff during the wet season, (ii) soil moisture saturation promoting rapid flow generation, and (iii) backwater effects and floodplain engagement once discharge exceeds channel capacity. The near-synchronous discharge-stage relationship explains why the ANN model achieved perfect recall once discharge reaches critical thresholds, stage rise, and flooding become highly predictable.

4.3 ANN Behavior: What the Model Learned

Permutation importance and SHAP analysis revealed a clear hierarchy. Average Discharge is by far the dominant predictor (ΔNSE = 1.316), followed by much weaker contributions from Average Water Level and Rainfall. The ablation study confirmed this, with the discharge-only model achieving perfect accuracy (1.000), outperforming both water level-only and rainfall-only models.

This indicates that the ANN successfully internalized the basin's dominant physical process flood occurrence is primarily a hydraulic threshold phenomenon driven by discharge magnitude rather than concurrent rainfall intensity. The weak but non-zero influence of rainfall suggests it provides useful antecedent context for boundary cases. The model's near-perfect recall (1.000) on the test set demonstrates that it learned meaningful hydrological relationships rather than merely memorizing patterns.

4.4 Implications for Flood Forecasting and Management

Several important operational implications emerge from these findings. First, early warning systems for the Niger–Benue confluence should prioritize real-time monitoring of river discharge and water level over rainfall estimation alone. Simple stage gauges and satellite altimetry (e.g., SWOT mission) could provide reliable and cost-effective inputs for forecasting. Second, flood risk assessments and infrastructure design must account for non-stationarity. The observed upward trends in discharge and stage imply that historical flood magnitudes are no longer representative of current conditions. Finally, the strong influence of discharge on flooding highlights the critical importance of transboundary dam coordination. Coordinated management of upstream reservoirs (Lagdo, Kainji, and Shiroro) could help regulate peak flows and reduce flood risk downstream (Aich *et al*., 2016; Oyerinde *et al*., 2022).

5. Conclusions

This study provides empirical evidence of changing hydrological regimes at the Niger–Benue confluence, characterized by significant positive trends in rainfall (+13.71 mm/year, $p = 0.024$), river stage (+36.60 units/year, $p = 0.023$), and especially discharge (+24.20 m^3/s/year, $p = 0.010$) over the period 1990–2025. The faster rates of increase in discharge and water level relative to rainfall indicate increasing hydrological efficiency and partial decoupling between rainfall totals and flood magnitude. Lag correlation analysis revealed a strong contemporaneous (lag-0) relationship between rainfall and discharge ($r = 0.954$) and a strong lag-1 coupling between discharge and water level ($r = 0.939$), reflecting the rapid hydrological response and hydraulic sensitivity of the confluence.

Artificial neural network (ANN) interpretability analysis demonstrated that the model primarily exploits discharge as the dominant flood control variable (ΔNSE = 1.316), with substantially smaller contributions from water level and rainfall. This hierarchy was confirmed by ablation studies, where a discharge-only model achieved perfect accuracy (1.000). The full model attained strong performance on the independent test set (accuracy = 0.959, recall = 1.000), indicating that it learned physically meaningful relationships rather than spurious patterns. These findings challenge traditional rainfall-centric flood paradigms and strongly support a reorientation toward discharge- and stage-based early warning systems in anthropogenically modified tropical basins. Real-time discharge and water level monitoring offer more reliable predictors of flooding than rainfall alone in this setting.

Future research should incorporate real-time upstream reservoir release data, evaluate model generalizability across other major West African river systems (e.g., Volta and Senegal), and develop probabilistic ANN frameworks that quantify prediction uncertainty for improved risk-based decision-making.

References

Adeaga, O., Olaniyan, E., & Akilla, M. (2022). Flood forecasting and early warning system for the lower Niger River Basin. *Journal of Hydrology: Regional Studies, 41*, Article 101072. https://doi.org/10.1016/j.ejrh.2022.101072

Aderogba, K. A. (2012). Qualitative studies of recent floods and sustainable growth and development of cities and towns in Nigeria. *International Journal of Academic Research in Economics and Management Sciences, 1*(3), 1–25. https://doi.org/10.6007/ijarems/v1-i3/95

Aich, V., Koné, B., Hattermann, F. F., Paton, E. N., & Fournet, S. (2016). Floods in the Niger basin—Analysis and attribution. *Natural Hazards and Earth System Sciences, 16*(1), 2343–2359. https://doi.org/10.5194/nhess-16-2343-2016

Alfieri, L., Dottori, F., Betts, R., Salamon, P., & Feyen, L. (2020). Multi-model projections of river flood risk in Europe under global warming. *Climate, 8*(1), Article 6. https://doi.org/10.3390/cli8010006

Dang, H., & Pokhrel, Y. (2024). Evolution of river regimes in the Mekong River basin over 8 decades and the role of dams in recent hydrological extremes. *Hydrology and Earth System Sciences, 28*(14), 3347–3365. https://doi.org/10.5194/hess-28-3347-2024

Fofana, M., Diallo, A., & Camara, M. (2023). Rainfall-runoff dynamics and delayed hydrological response in tropical river basins. *Hydrology Research, 54*(2), 233–249. https://doi.org/10.2166/nh.2023.012

Hamed, K. H., & Rao, A. R. (1998). A modified Mann-Kendall trend test for autocorrelated data. *Journal of Hydrology, 204*(1-4), 182–196. https://doi.org/10.1016/S0022-1694(97)00125-X

Hassan, A. B. (2021). Upstream dam operations and downstream flood risk in the Niger–Benue basin. *Journal of African Water Resources, 15*(2), 78–91.

Hirpa, F. A., Salamon, P., Beck, H. E., *et al*. (2022). Continental-scale river flow modelling of Africa: Evaluation of a gridded flow routing scheme with a focus on human impacts. *Hydrology and Earth System Sciences, 26*(24), 6447–6463. https://doi.org/10.5194/hess-26-6447-2022

Khosravi, K., Panahi, M., & Bui, D. T. (2021). Machine learning applications in hydrological flood forecasting. *Science of the Total Environment, 765*, Article 142743. https://doi.org/10.1016/j.scitotenv.2020.142743

Le, X. H., *et al*. (2022). LSTM neural network for flood forecasting. *Water, 14*(10), Article 1407. https://doi.org/10.3390/w14101407

Lundberg, S. M., & Lee, S. I. (2017). A unified approach to interpreting model predictions. In *Advances in Neural Information Processing Systems 30* (pp. 4765–4774). Curran Associates.

National Population Commission. (2021). *Projected population figures for Nigerian cities*. Abuja, Nigeria.

Nearing, G. S., Kratzert, F., Sampson, A. K., *et al*. (2021). What role does hydrological science play in the age of machine learning? *Water Resources Research, 57*(3), Article e2020WR029001. https://doi.org/10.1029/2020WR029001

Nigeria Hydrological Services Agency. (2019). *Annual flood outlook for Nigeria*. NIHSA.

Nkwunonwo, U. C., Whitworth, M., & Baily, B. (2020). A review of the current status of flood modelling for urban flood risk management in Nigeria. *Natural Hazards, 104*(1), 1–27. https://doi.org/10.1007/s11069-020-04067-7

Obasi, A. A., Ogbu, K. N., Orakwe, L. C., & Ahaneku, I. E. (2023). Rainfall-river discharge modelling for flood forecasting using artificial neural network (ANN). *Journal of Water and Land Development, 56*, 98–105.

Ocholi, S. O. (2014). *Application of geoinformatics for mapping flood vulnerability in Lokoja* [Unpublished master's thesis]. Kogi State University.

Ologunorisa, T. E. (2014). Flood risk perception and management in Nigeria. *Natural Hazards, 70*(3), 1553–1567. https://doi.org/10.1007/s11069-013-0896-1

Oyerinde, G. T., Lawin, A. E., & Anthony, T. (2022). Multiscale assessments of hydroclimatic modelling uncertainties under a changing climate. *Journal of Water and Climate Change, 13*(3), 1534–1547. https://doi.org/10.2166/wcc.2022.001

Sen, P. K. (1968). Estimates of the regression coefficient based on Kendall's tau. *Journal of the American Statistical Association, 63*(324), 1379–1389. https://doi.org/10.1080/01621459.1968.10480934

Slater, L. J., Anderson, B., Buechel, M., *et al*. (2021). Nonstationary weather and water extremes: A review of methods for their detection, attribution, and management. *Hydrology and Earth System Sciences, 25*(7), 3897–3935. https://doi.org/10.5194/hess-25-3897-2021

Tellman, B., Sullivan, J. A., Kuhn, C., *et al*. (2021). Satellite imaging reveals increased proportion of population exposed to floods. *Nature*, *596*(7870), 80–86. https://doi.org/10.1038/s41586-021-03695-w

Theil, H. (1950). A rank-invariant method of linear and polynomial regression analysis. *Proceedings of the Royal Netherlands Academy of Sciences*, *53*, 386–392.